Physiology & Behavior 276 (2024) 114460

Contents lists available at ScienceDirect

Physiology & Behavior

journal homepage: www.elsevier.com/locate/physbeh

Integrative neuro-cardiovascular dynamics in response to test anxiety: A brain-heart axis study☆

Vincenzo Catrambone [*,a], Lorenzo Zallocco [b], Eleonora Ramoretti [b], Maria Rosa Mazzoni [b], Laura Sebastiani [1,b,c], Gaetano Valenza [1,a]

[a] Neurocardiovascular Intelligence Laboratory, Department of Information Engineering & Bioengineering and Robotics Research Center E. Piaggio, School of Engineering, University of Pisa, Pisa, Italy
[b] Department of Translational Research and New Technologies in Medicine and Surgery, University of Pisa, Pisa, Italy
[c] Institute of Information Science and Technologies A. Faedo, ISTI-CNR, Pisa, Italy

ARTICLE INFO

Keywords:
Brain-heart interplay
EEG
Heart rate variability
Test anxiety

ABSTRACT

Test anxiety (TA), a recognized form of social anxiety, is the most prominent cause of anxiety among students and, if left unmanaged, can escalate to psychiatric disorders. TA profoundly impacts both central and autonomic nervous systems, presenting as a dual manifestation of cognitive and autonomic components. While limited studies have explored the physiological underpinnings of TA, none have directly investigated the intricate interplay between the CNS and ANS in this context. In this study, we introduce a non-invasive, integrated neuro-cardiovascular approach to comprehensively characterize the physiological responses of 27 healthy subjects subjected to test anxiety induced via a simulated exam scenario. Our experimental findings highlight that an isolated analysis of electroencephalographic and heart rate variability data fails to capture the intricate information provided by a brain-heart axis assessment, which incorporates an analysis of the dynamic interaction between the brain and heart. With respect to resting state, the simulated examination induced a decrease in the neural control onto heartbeat dynamics at all frequencies, while the studying condition induced a decrease in the ascending heart-to-brain interplay at EEG oscillations up to 12Hz. This underscores the significance of adopting a multisystem perspective in understanding the complex and especially functional directional mechanisms underlying test anxiety.

1. Introduction

Social anxiety is the second most common anxiety disorder with a lifetime prevalence of 6.7%–10.7% in western countries [1]. Social anxiety is commonly referred to as a human experience characterized by the belief of being constantly exposed to the judgment of others, with the resulting expectation and fear of being judged negatively [2]. Most people feel a sense of vulnerability and fear when faced with important events that require them to demonstrate their abilities or when they are the center of attention. This fear can sometimes also be positive, but when the fear is severe and pervasive, pathology may begin [3,4]. A specific form of social anxiety is *test anxiety*, described as "the set of phenomenological, physiological, and behavioral responses that accompany concern about possible negative consequences or poor performance on an examination or a similar evaluative situation" [5]. One widely accepted view defines test anxiety as a situational personality trait characterized by persistent worry, intrusive thoughts, mental disorganization, tension, and physiological arousal during evaluation situations [6,7]. Two central components of test-related anxiety have been outlined [8]: the cognitive component, prominently featuring "concern," and the second component, termed "emotivity," which encompasses physiological, autonomic-related responses such as increased heart rate, sweating, dry mouth, shortness of breath, and nausea. Notably, the cognitive "concern" component exerts a greater impact on

☆ This research has received partial funding from the University of Pisa in the framework of the PRA 2020-2021 project awarded to G.V. and L.S., and Italian Ministry of Education and Research (MIUR) in the framework of FoReLab ad CrossLab projects (Departments of Excellence), and PNRR under the Project THE (cod. ECS00000017 - CUP I53C22000780001).

* Corresponding author.
E-mail address: vincenzo.catrambone@unipi.it (V. Catrambone).
[1] Senior authors.

https://doi.org/10.1016/j.physbeh.2024.114460
Received 19 October 2023; Received in revised form 8 December 2023; Accepted 8 January 2024
Available online 10 January 2024

performance compared to the physiological "emotivity" component [9]. In extreme cases, the anxiety may lead to episodes in which persons experience anxious/panicked state [10], e.g. high anxiety during MRI-related claustrophobia with a high respiratory rate [11,12].

The brain regions primarily implicated in social anxiety encompass those associated with emotional processing, higher cognitive functions related to emotion regulation, and behavioral responses to stimuli [13]. These include the amygdala, along with interconnected structures such as the prefrontal cortex, fusiform gyrus, insula, inferior frontal gyrus, and superior temporal sulcus [3,14–18]. While most of the identified brain regions consistently belong to the central autonomic network (CAN) [3,19] - including brain regions linked to the autonomic nervous system (ANS) control - the aforementioned two-component definition of test-related anxiety [8] posits the coexistence of cognitive and autonomic components. Nevertheless, the continuous and multipath interplay between the CNS and the ANS, often referred to as the functional brain-heart interplay (BHI) [20], has not been previously explored in the context of test anxiety.

To this end, this study introduces a multi-system analysis examining the dynamic behavior of central nervous system (CNS) and ANS, utilizing electroencephalography (EEG) and heart rate variability (HRV) series analysis, along with an assessment of their functional interaction. Quantification of functional BHI has been a topic of increasing interest in the scientific community in recent years. From a purely methodological point of view, this problem faces a number of technical difficulties, being intrinsically multimodal and multivariate. There is also the issue of directionality, meaning that brain-toheart interactions are not necessarily the same as heart-tobrain interactions, and that physiological plausibility must be considered when using classical signal processing tools. However, several methodologies have been applied or specifically developed to estimate BHI. Information theory quantifiers have been developed to capture both linear [21] and nonlinear interactions [22]. In addition, measurement methods such as an point process-based transfer entropy have been devised to target scalp activity instantaneous influence onto heart rate [23]. In addition, heartbeat evoked potentials investigated the overall response of the scalp to the heartbeat, which is perceived as an interoceptive stimulus [24]. Other studies have proven that BHI extends to multifractal regimes [25] or explored the complexities of cerebrovascular dynamics [26,27], and a method was specifically developed to detect microstates, i.e., quasi-stable states, of brain-heart axis dynamics [28]. Although these studies demonstrated the feasibility and high impact of combined brainheart interplay assessment, we believe that a physiologically plausible multivariate modelling allowing for an ad hoc, fully parametric directional estimation of BHI is the most suitable solution.

In this study, we utilize the Synthetic Data Generation model (SDG) [29] to estimate functional BHI from EEG and ECG series. Remarkably, the SDG model implementation is publicly available and its physiologically-plausible equations have profitably been exploited for the characterization of emotion perception [30], neuroautonomic maneuvers [31], and subclinical depression [32], among others. It is also important to note that there is no scientific consensus on which method should represent the standard quantifier for BHI, and some methods may be more appropriate in certain situations. Here, a BHI assessment has been performed in healthy subjects experiencing experimentally-induced test anxiety, which is compared to a resting state. The hypothesis posited here is that test anxiety induces a characteristic variation in the directional (afferent or efferent) BHI, distinct from rest, not solely explicable by individual CNS or ANS dynamics, but rather by their interplay.

2. Materials and methods

2.1. Experimental dataset

The study involved 27 voluntary healthy young students from the University of Pisa (mean age: 23.7 ± 3.2 years). Participants were required to have no prior history of neurological, psychiatric, or medical conditions to meet the inclusion criteria. Initially, participants underwent an extensive questionnaire session, including psychometric measurements for evaluating social anxiety, such as the Leibowitz scale. The questionnaires further included assessments through the Social Phobia Scale (SPS), the Social Inventory Scale (SIAS), the Westside Test Anxiety Scale, the Italian Social Phobia Inventory (I-SPIN), and the Brief Social Phobia Scale (BSPS). Additionally, participants' general anxiety levels were e valuated through the Trait Anxiety Scale (STAI-Y2) and the Hamilton Anxiety Scale (HAS). Then, they received a concise explanation of the experimental procedures and provided informed consent.

Participants were then seated in a comfortable armchair and equipped with the g-Nautilus 32 Multi-purpose System (gTech, Austria) to record synchronized EEG and ECG signals. The experimental protocol began with an initial 10-minute resting state with closed eyes. Subsequently, three consecutive sessions were conducted: relaxation (R, 2 min), study (S, 3 min), and interrogation (I, approximately 2 min). In the relaxation phase, participants were instructed to relax with open eyes on a semi-reclined armchair, listening to the sound of waves through headphones. At the end of this phase, subjects completed the Italian version of the STAI Y1 questionnaire on state anxiety [6]. During the study phase, volunteers read and memorized a written text containing information outside their field of study, including dates and proper names. At the session's conclusion, participants completed the Italian version of the Speech Preparation Questionnaire (PREP) [33], assessing confidence, nervousness, calmness, preparedness, and anticipated performance. PREP questionnaire is a 5-item self report questionnaire assessing, on a Likert scale 0-5 (0 = extremely low; 5 = very high), the confidence, nervousness, calmness, and preparedness of an individual before he/she gives the oral presentation. Participants were also required to "predict" the goodness of their performance on a Likert scale 0-5 (0 = very bad; 5 = very good).

During the interrogation phase, subjects were asked to speak about the studied text in front of a "professor", with the elapsed time displayed on the screen. They were informed that the professor would assess their performance in terms of knowledge retention, accuracy, and verbal fluency on a 30-point scale, consistent with the Italian university's exam scoring. The session concluded after 2 min or if the participant paused for more than 5 s or expressed an inability to recall further details. The state STAI Y1 questionnaire was completed afterward, and participants were then informed of the study's true purpose. A block diagram of the experimental protocol implemented is reported in Fig. 1.

Physiological recordings included a 17-channel EEG, referenced to CZ, and electrocardiogram (ECG), all sampled at 500 Hz. The ethical committee of the University of Pisa approved the study (Approval No. 1/2021, dated 29/01/2021), conducted in accordance with the ethical standards outlined in the Declaration of Helsinki.

2.2. EEG processing

The EEG signal processing followed a standard pipeline [34], which involved several steps:

1. Normalization and Channel Quality Check: The normalized mean joint probability of the log-power from 1 to 70*Hz* was computed. Channels in the outer 1% distribution tails were identified as corrupted.
2. Band-pass Filtering: EEG series were band-pass filtered below 0.5*Hz* and above 45*Hz* using multi-taper regression to remove high and low frequency electrical noise.
3. Artifact Removal and Component Analysis: A wavelet-enhanced independent component analysis (wICA) was applied for the detection and rejection of eye and muscle activity, as well as discontinuities. A machine learning algorithm was also employed to identify artifacts from wICA-derived components [34].

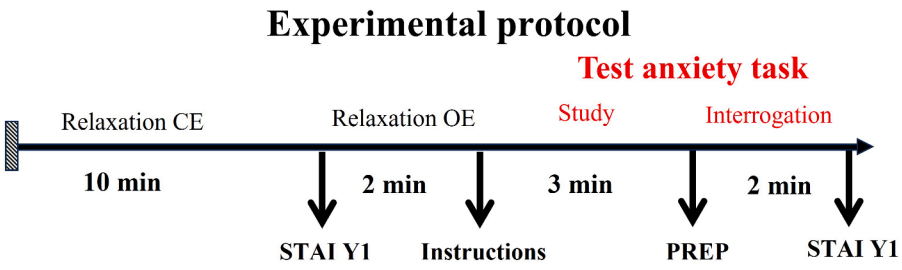

Fig. 1. Block diagram of the experimental protocol pipeline. CE: closed eyes. OE: open eyes.

4. Channel Restoration: A spherical interpolation algorithm was used to recover rejected channels by utilizing neighboring EEG data.
5. Re-referencing: The time-varying average of all channels was derived for re-referencing the EEG series (i.e., average referencing).

The power spectral density (PSD) of the EEG channel was estimated using Welch's method. Specifically, a Hamming window of 1000 samples (2*s*) with a step size of 125 samples (250*ms*) was applied to achieve acceptable time resolution. The resulting PSD was then filtered to obtain the power time course in the four standard frequency bands: delta band δ from 0.5 to 4*Hz*; theta band θ from 4 to 8*Hz*; alpha band α from 8 to 12*Hz*; and beta band β from 12 to 30*Hz*. All preprocessing steps were carried out using MatLab software and the EEGLAB toolbox [35].

2.3. ECG processing

HRV series were obtained from ECG signals using the well-known Pan-Tompkins algorithm [36]. These series were preprocessed to eliminate artifacts and erroneous R-beats through a point-process-based algorithm [37]. Subsequently, the derived HRV series underwent visual inspection to ensure validity.

The power spectral density (PSD) estimation of HRV seris was performed using the smoothed pseudo-Wigner-Ville distribution, with a time resolution synchronized with that of the EEG-PSD. The resulting PSD series were then integrated into the canonical low frequency (LF, [0.04–0.15] *Hz*) and high frequency (HF, [0.15–0.4] *Hz*) bands.

2.4. BHI estimation

To estimate functional BHI, we utilized the Synthetic Data Generation model (SDG) [29]. This model has previously been employed in studies related to emotion perception [30], autonomic maneuvers [29], and mood disorders [32].

Formally, the EEG-HRV multivariate system is represented by multiple oscillators (one for each considered frequency band in the EEG), where the amplitudes are calculated using a first-order exogenous autoregressive model for the EEG side [24]. This model accounts for time-resolved communication from the heart to the brain through an exogenous term. On the HRV side, the time series is modeled using an integral pulse frequency modulation model [38]. Here, the direction-specific brain-to-heart coupling is mathematically formalized through an exogenous term added to the function representing autonomic activity.

In summary, heart-to-brain and brain-to-heart interactions are extracted for each combination of EEG and HRV frequency components as time-varying directional BHI biomarkers. The SDG model is founded on the notion that the electrophysiological activity of both systems (CNS and ANS) are functionally interdependent, and the mathematical formulation aims to capture this relationship. For instance, a positive value of $C_{\alpha \to HF}(t_n)$ indicates that the α band of the EEG-PSD at time t_n positively influences (i.e., induces a linear increase in) the HRV-PSD series in the HF band.

For a comprehensive mathematical formulation of the model, the interested reader may refer to [29,32]. A MATLAB implementation is freely available at [39].

To assess the statistical significance of the extracted BHI estimates, we implemented two different approaches employing surrogate data analysis [40]. The first was developed randomizing the PSD time series, performing time-shuffling. Following this procedure in deriving a specific BHI index, e.g. the θ-to-LF BHI index, we randomly shuffled the θ-PSD and LF-HRV-PSD as input of the SDG model and run the simulation 100 times. Significance was determined by checking if the true BHI index value belonged to the 5% most external tails of the BHI index distribution derived by the surrogate data analysis. It has to be noted that the derived BHI indexes might assume both positive and negative values, with negative values obtained when an increase of the driver signal results in a decrease in the target one. The second approach implemented a different type of randomization. Considering, e.g., a brain-to-heart assessment, we associate EEG series of a given subject to cardiovascular variability series of a different subject and/or different experimental phases [40]. This allows to preserve all the time and spectral properties of an input (i.e., an EEG-PSD time series) and output series (i.e., a HRV-PSD). More specifically, our data from 27 healthy volunteers undergoing three different experimental phases (i.e., resting, studying, and interrogation) provides a total of $27 \times 3 = 81$ experimental series. To run the surrogate data analysis, we extracted the BHI on all possible combination of 81 EEG series with all the 80 HRV series, thus excluding from the null distribution the combinations representing the true original pairs. This procedure was repeated for all EEG- and HRV- frequency bands, as well as for all EEG channels. If the original estimate was more external than the 5% tail of the null distribution, the estimate was deemed significant and retained for further analyses.

2.5. Group-wise feature extraction and statistical analysis

Feature extraction comprised the following three feature sets:

- EEG power: time-resolved estimation of the EEG power in the δ, θ, α, andβ bands.
- HRV power: time-resolved estimation of the HRV power in the LF and HF bands.
- functional BHI: time-resolved estimation of the directional BHI as tabulated in Table 1.

For each experimental condition, a time-resolved estimation was averaged across time to obtain one feature per subject/condition. Accordingly, in each domain (EEG power, HRV power, functional BHI), the statistical analysis encompassed non-parametric tests for paired samples. This involved group-wise comparisons through the Friedman

Table 1
BHI indices extracted through the model.

Index	From	Band	To	Band
$C_{Brain_j \to Heart_{B_iC}}$	Brain	$\delta, \theta, \alpha, \beta$	Heart	LF, HF
$C_{Heart_{B_iC} \to Brain_j}$	Heart	LF, HF	Brain	$\delta, \theta, \alpha, \beta$

test, comparing the *R* vs. *S* vs. *I* phases, as well as pair-wise comparisons for all possible pairs of experimental phases, employing the Wilcoxon test for paired samples.

Group-wise comparisons were assessed with a significance level of $\alpha = 0.05$, while the pair-wise comparisons were corrected using Bonferroni-Holm correction. Furthermore, to account for multiple EEG-channel comparisons and ensure physiological plausibility of the obtained results, a spatial cluster permutation correction was applied [41].

3. Experimental results

The psychometric questionnaire results have been summarized in Tables 2 (Leibowitz Scale), 3 (STAI - comprising both STAI Y2 and Y1), and 4 (PREP questionnaire).

A pairwise statistical comparison was performed on the scores obtained from the state anxiety scale (STAI Y1) before and after the task. This analysis unveiled a highly significant difference (Post-task > Pre-task, p-value < 0.001), indicating an increased level of anxiety induced by the experimental stimuli. The high level of induced anxiety did not lead to any panic attack, which would significantly change the physiological responses. While Table 3 shows a mean STAIY1 score of 13.6296 for the difference between post- and pre-test, Fig. 2 shows the violin boxplot of STAIY1 values, both pre- and post- test, as well as their difference. We can appreciate that such delta in the STAIY1 collected values has its maximum lower then 40, and its minimum close to zero.

3.1. Electroencephalography (EEG)

Fig. 3 provides a topographical representation of the statistical analysis results on EEG-PSD data. In the group-wise comparison, a broad statistically significant region in the δ frequency band was observed, spanning from anterior to posterior regions, with the exception of a right temporal and a left fronto-temporal area. In the θ band, statistically significant regions included the Fp1 and Fp2 frontal electrodes, along with a centro-parietal right region. Notably, these regions also showed enhancement in the analysis of the α frequency band. In the β band, only a frontal right cluster exhibited statistical significance.

The pairwise statistical comparison did not reveal any significant differences when comparing the relaxation phase to either the studying or interrogation phase. Conversely, in the δ band, nearly the entire scalp exhibited significance when comparing the studying phase to the interrogation phase, with the exception of both left and right temporal distal electrodes and a single fronto-central one. In the α band, a bilateral parieto-occipital region together with a right frontal area were found to be significant. In the β band, only the right frontal electrodes remained significant. Notably, all the electrodes highlighted as significant in panel (d) of Fig. 3 (i.e., the comparison between studying and interrogation phases) indicate an increased EEG-PSD when transitioning from the studying to the interrogation phase.

3.2. Heart rate variability

Significant changes among experimental conditions in HRV analsys were observed, as illustrated in Fig. 4. Specifically, the transition from relaxation to the studying phase led to an increase in HRV-PSD in the LF band. The non-parametric Wilcoxon test for paired samples yielded a p-value of 0.0061, indicating significance. This increase persisted during the interrogation phase, where the statistical comparison between relaxation and interrogation resulted in a p-value of 0.021. Although the median LF power was higher during interrogation compared to the studying phase (see Fig. 4), this difference was not statistically significant.

In the HRV-HF band, which may serve as a biomarker of vagal activity, the only statistically significant comparison was between relaxation and studying phases (p-value of 0.0142). Here, the latter phase exhibited a slight decrease in HF power compared to the former. Notably, the overall decrease observed in the HF band during the studying phase was partially compensated in the last experimental phase (interrogation), which, however, was not significantly different compared to the previous two.

The analysis of the LF/HF ratio leads to similar results as the LF

Table 2
Statistical characterization of the response collected on the Leibowitz Scale. MAD: mean absolute deviation.

Leibowitz Scale					
	Performance		Social Anxiety		
	anxiety	avoidance	anxiety	avoidance	total
Median	13	9	11	10	43
MAD	5.17	5.91	4.71	5.42	21.21

Table 3
Statistical characterization of the response collected through STAI questionnaire. MAD: mean absolute deviation.

	STAI Y2	STAI Y1		Δ STAI Y1
	Trait	pre-task	post-task	Post-Pre
Median	53	33	47	10
MAD	8.89	4.56	9.16	8.30

Table 4
Statistical characterization of the response collected through PREP questionnaire. SD: standard deviation.

PREP Measure	Mean	SD
Nervous	3.56	1.003
Confident	2.28	1.021
Calm	2.08	0.812
Prepared	2.36	0.907
Estimation of performance	2.12	0.833

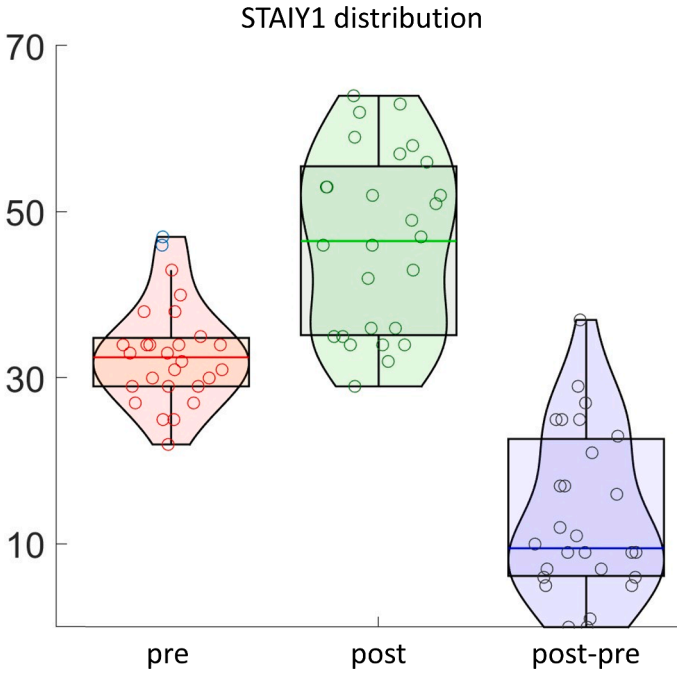

Fig. 2. Graphical representation of results on STAIY1 data. Violin boxplots depict the distribution of STAIY1 collected in each experimental phase (pre-experiment in red on the left, post experiment in green at the center of the figure, and the difference between post- and pre- phase, on the right depicted in blu).

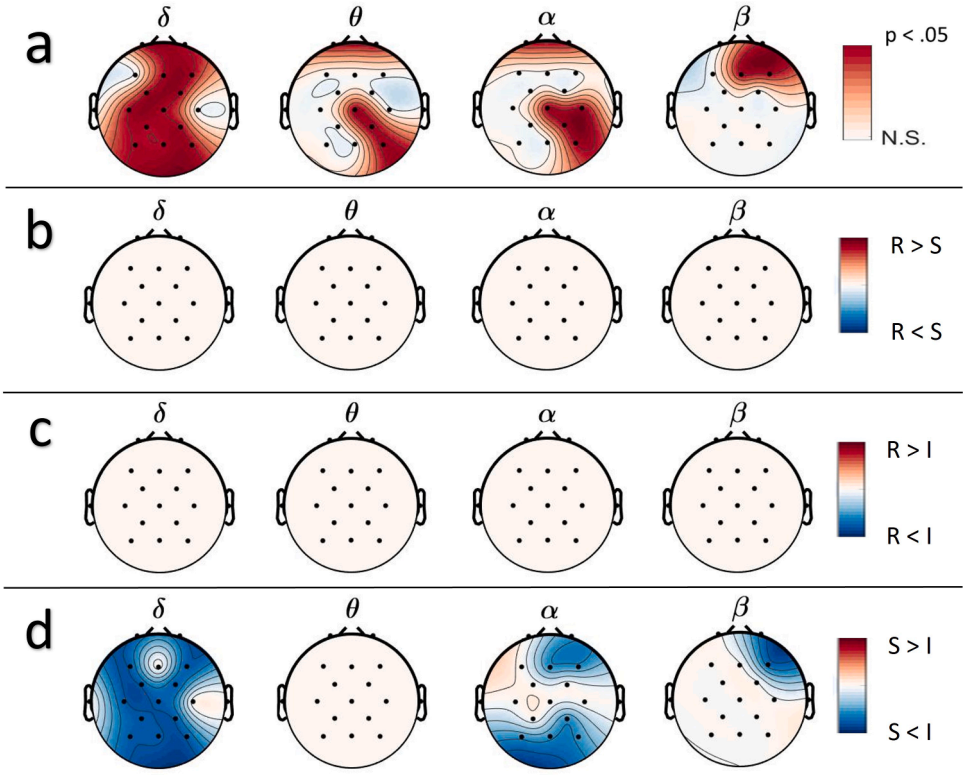

Fig. 3. Topographical representation of statistical analysis results on EEG-PSD data. Each column reports on a specific frequency band, from left to right: delta δ, theta θ, alpha α, and beta β. The first row (a) displays the results of the Friedman test, with statistically significant regions shown in red, and non-significant electrodes in white areas. Rows two through four depict pair-wise statistical comparisons results. (b) Relaxation (R) vs. Studying (S) phase. (c) Relaxation (R) vs. Interrogation (I) phase. (d) Studying (S) vs. Interrogation (I) phase. In the last three subpanels, white areas denote non-significant regions, electrodes where the first term exhibits a statistically significant higher median than the second term are depicted in red, and the opposite is shown in blue.

index, with lower *p*-values. Specifically, the transition from relaxation to the studying phase led to a significant increase (*p*-value of 0.0003), which is maintained during the interrogation phase, where the statistical comparison between relaxation and interrogation resulted in a *p*-value of 0.0001. Although the median LF/HF ratio was higher during interrogation compared to the studying phase (see Fig. 4), this difference was not statistically significant.

All the statistical analysis performed on average heart rate (expressed in bpm) lead to significant differences with *p*-values always lower than $10^{-}4$. From Fig. 4 it appears evident that there is a progressive increase in the heartbeat average interval length from the relaxation phase to studying phase, which continues to increase in the interrogation phase.

3.3. Brain-heart interplay

All BHI estimates, from various EEG channels, EEG and HRV frequency bands, and the two BHI directions, were found to be statistically significant across all subjects through the first surrogate data analysis method. Additionally, more than 95% of the BHI estimates were retained for further analyses based on the results obtained from the second surrogate data analysis method. The analysis of statistically significant BHI dynamics revealed several changes among experimental conditions, as depicted in Fig. 5 through the topographical distribution of significant *p*-values. In the group-wise paired comparison, utilizing the non-parametric Friedman test, bidirectional BHI changes were observed when considering cardiac oscillations in the HRV-LF band functionally linked with all EEG frequency bands, except for the heart-to-brain LF-β pair (see Fig. 5a). Brain-to-heart comparison was significant in all EEG frequency bands, particularly involving frontal, central, and parietal regions. However, bilateral distal temporal regions, as well as a left fronto-temporal electrode, appeared unaffected by the experimental elicitation. Occipital lobes showed significant differences among groups in brain-to-LF pairs considering $\delta, \theta,$ and α frequency bands, but not the β range. A detailed examination of the brain-to-LF interaction suggests that the significant comparisons (see Fig. 5) are primarily driven by a substantial decrease during the interrogation phase, as no differences were detected when comparing relaxation with studying (Fig. 5b). Both relaxation VS interrogation (Fig. 5c) and studying VS interrogation (Fig. 5d) revealed significant and widespread differences with positive sign.

Notably, the descending interplay between central and autonomic activity showed no difference in the group-wise comparison, nor in any of the pair-wise statistical tests involving the vagal HF component.

The directional BHI in the ascending direction (i.e., heart-to-brain) showed significant sensitivity to experimental changes across various combinations of EEG- and HRV-derived frequency bands (see Fig. 5). In the group-wise comparison, all frequency bands demonstrated physiological involvement, except for the EEG-β range, which exhibited no significant change across experimental phases, whether considering LF or HF frequency bands.

Significant group-wise variations were observed in the LF-to-brain interplay, particularly in relation to δ (excluding distal temporal electrodes), α (in a frontal centro-left region and a diffuse dorso-central, parietal, and occipital region), and θ EEG bands. Notably, θ displayed slightly higher (yet still significant) *p*-values along the vertical axis (from frontal to occipital electrodes). These changes were attributed to a significantly lower LF-to-brain interplay during the studying phase compared to both relaxation and interrogation phases, particularly in regard to δ and θ EEG bands. Specifically, low-frequency cortical EEG components (δ and θ) and cardiovascular LF exhibited significantly lower ascending BHI in the studying phase compared to the relaxation

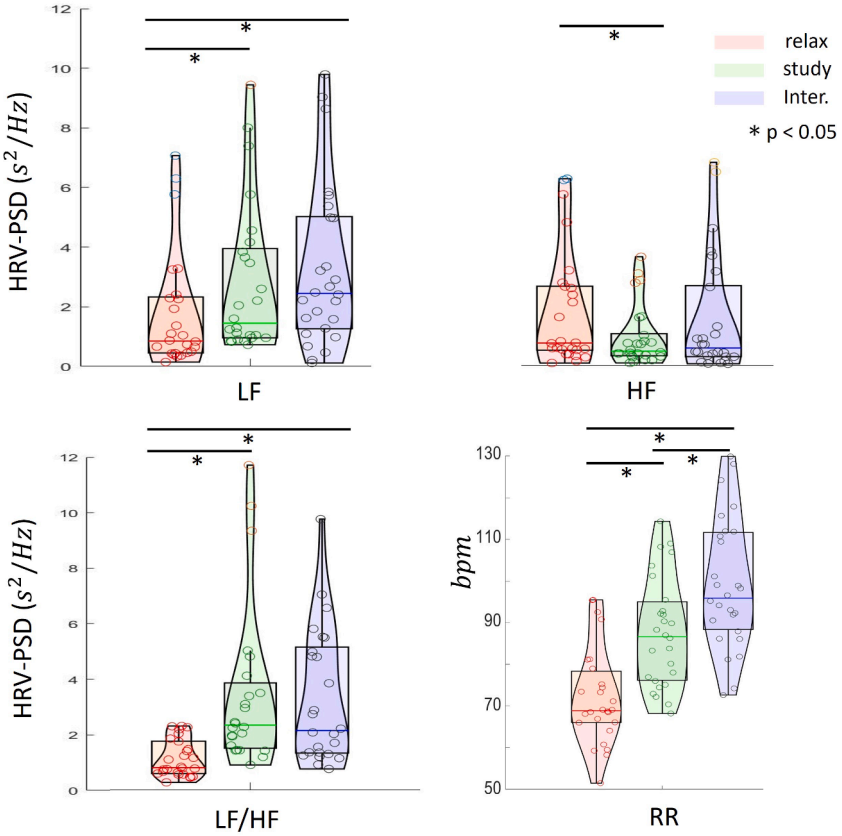

Fig. 4. Graphical representation of results on HRV data, along with associated statistical analysis. Violin boxplots depict the distribution of HRV-PSD detected in each experimental phase (relaxation in red, studying in green, interrogation in blue). The top-left part of the figure represents HRV-LF band, while HRV-HF band is shown on the top-right. In the bottom part of the figure, on the left the LF/HF ratio results are presented, whereas on the right the average heartbeat time intervals are reported. Asterisks indicate statistically significant comparisons.

phase (see Fig. 5b), as well as significantly lower ascending BHI in the interrogation phase (see Fig. 5d).

Conversely, significant BHI changes in the LF-to-α combination were only observed in the relaxation VS studying phase comparison and did not manifest in other statistical comparisons. A similar trend was noted for HF-to-brain interplay, as the statistically significant comparisons observed in the group-wise analysis (Fig. 5a) were only evident in the pair-wise relaxation VS studying phase comparison, not in other experimental comparisons (with the exception of a significant increase in a cluster of two electrodes in the HF-to-θ combination in the studying VS interrogation comparison reported in Fig. 5d).

4. Discussions and conclusions

This study provide a thorough investigation of synchronized neural and cardiovascular dynamics, as well as their interplay, during test anxiety. Test anxiety was induced in a group of healthy student volunteers through an experimental protocol involving an interrogation session in front of a professor. This was preceded by a brief studying phase following an initial relaxation period. Physiological correlates were evaluated using PSD-derived measures of central activity (through EEG recordings) and autonomic activity (via HRV series). The functional interaction between these measures was investigated using the BHI SDG estimation model [29].

The results on self-assessment reports demonstrated that the administered protocol successfully induced test anxiety, which aligned with findings from a previous study where test anxiety was induced using the same protocol [42]. Specifically, following the studying phase, all participants reported elevated levels of nervousness coupled with low expectations regarding their performance outcome (as indicated by the PREP questionnaire results in Table 4). Furthermore, after the interrogation phase, participants reported significantly higher levels of perceived anxiety compared to the post-relaxation period. Nonetheless, it has been assured that the perceived anxiety did not overcome to panic attacks. Those are events that might be related to test anxiety and the associated physiology, which is still under investigation, strongly affect the activity and the interaction of cardiovascular, respiratory and brain systems [10–12].

Analysis of cardiac autonomic activity revealed significant differences between the studying and relaxation phases, highlighted in both LF and HF power components of HRV. Additionally, differences were observed between the interrogation and relaxation phases, particularly in relation to the LF band. The absence of significant changes in HF power suggests that participants were able to effectively cope with the cognitive demands of the task even in the presence of test anxiety. This aligns with the notion that a reduced decrease in cardiac vagal activity during tasks involving executive functioning can be considered adaptive [43], and has been linked to enhanced task performance [44]. Conversely, the interrogation phase significantly affected cardiac vagal activity. This may be speculatively due to changes in respiration patterns induced by speaking [45,46]. However, the expected nature of this alteration is a topic of debate. Indeed, some studies on verbal stress tasks, such as speech tasks [47], have reported a reduction in respiration rate [46], while others have noted an increase in respiratory frequency [48], and some found no significant differences [45]. It has been shown that natural nasal breathing synchronize electrical activity in human piriform cortex and limbic related brain areas including amygdala and hippocampus, and when breathing was changed from nose to mouth this effect disappeared [49]. Nevertheless, it seems plausible to consider that speaking during verbal stress tasks might introduce a confounding effect

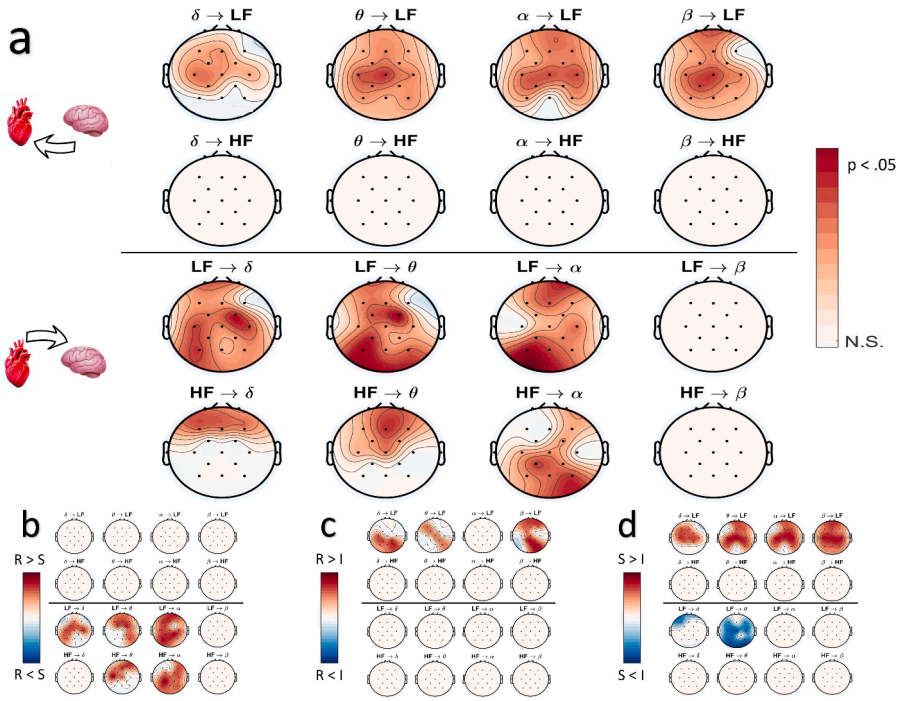

Fig. 5. Topographical representation of statistical analysis results on BHI data. In each subpanel, columns refer to specific EEG frequency bands, from left to right: delta δ, theta θ, alpha α, and beta β. The first two rows refer to brain-to-heart interplay (HRV-LF on top), while the last two rows of each subpanel refer to heart-to-brain interplay (HRV-LF first, followed by HRV-HF). Subpanel (a) displays the results of the Friedman test, with statistically significant regions shown in red, and non-significant electrodes in white areas. The other subpanels represent pair-wise statistical comparison results. (b) Relaxation (R) vs. Studying (S) phase. (c) Relaxation (R) vs. Interrogation (I) phase. (d) Studying (S) vs. Interrogation (I) phase. In the last three subpanels, white areas indicate non-significant regions, electrodes where the first term exhibits a statistically significant higher median than the second term are depicted in red areas, and the opposite is shown in blue.

that could potentially obscure or diminish vagal withdrawal.

EEG power analysis unveiled cortical activity shifts primarily occurring between the studying and interrogation phases. These changes manifested as diffuse alterations observed across the scalp in the δ and α EEG bands, along with more localized modifications in the θ and β bands. In terms of frequency domain considerations, our experimental protocol was designed to replicate conditions as closely as possible to a real-life scenario (such as taking an oral exam with limited time for preparation). This situation necessitates the engagement and coordination of multiple brain networks involved in language processing, learning, memory, and social anxiety. These activities are reflected through oscillations in various EEG frequency bands. For instance, studies have demonstrated that oscillations in the δ and θ range are particularly sensitive for word reading and the integration of words into meaningful chunks, both during reading and speech production [50]. The θ band is also known to play a role in visual attention [51–53] and episodic retrieval [54]. Moreover, numerous studies have indicated the modulatory effect of anxiety on various EEG bands, such as δ and β in response to speech anticipation [33]. Additionally, an increase in EEG α power has been associated with high-anxiety traits during attentional tasks [55], and an uptick in β activity has been considered an expression of attentional top-down modulation in conditions of psychosocial stress [56]. Therefore, the engagement of EEG oscillations spanning across extensive brain regions and frequency ranges, which resonates in the reciprocal interplay between brain and heart, is not unexpected. This underscores the necessity of intricate brain activity and brain-body interactions to uphold the cognitive and emotional facets of the test anxiety experience.

The directional brain-heart analysis offers an original perspective on the physiological responses induced by test anxiety. Specifically, it reveals that the distinctions between relaxation and studying primarily occur in an ascending (heart-to-brain) direction, involving cardiovascular oscillations in the LF and HF frequency bands. Conversely, differences between relaxation and interrogation manifest in a descending (brain-to-heart) direction, limited to the LF HRV band. The lower end of the cardiovascular functional spectrum is bidirectionally implicated in the comparison between studying and interrogation, with the entire scalp and spectrum affected by the BHI decrease detected in the descending direction. Meanwhile, only the δ and θ EEG frequency bands, in localized areas, are involved in the BHI increase detected in the ascending heart-to-brain direction. These results on the brain-heart axis activity are in line with the fact that test anxiety induces both cognitive and autonomic responses.

Comparing with prior findings, BHI complex dynamics is known to be modulated by a cognitive task, such as mental arithmetic, compared to a resting state [27]. These changes are confined to the LF-to-brain direction and in the δ, θ, and α bands, with no alterations in the LF-to-β combination [27]. This aligns with the findings in the LF-to-brain interplay in this study (refer to Fig. 5). It is then plausible to argue that the LF-to-brain decrease detected during the studying phase, in comparison to both relaxation and interrogation, may be associated with the cognitive component induced by the protocol administered in this study.

Additionally, the heart-to-brain changes, particularly in the HF-to-brain, and the brain-to-LF elicitation reported here, correspond with what was observed in [57]. In that study, an autonomic maneuver like the cold pressor test induced both sympathetic and parasympathetic variations in the heart-to-brain ascending interaction. In contrast, a pure sympathetic change was noted in the descending brain-to-heart interplay. Emotional elicitation also results in a bidirectional BHI, with a swifter response from the ascending modulation [30], a reaction known to involve both cognitive and autonomic aspects.

Further investigations are warranted to potentially establish a connection between the brain-to-LF behavior observed in this study and the autonomic sympathetic variations reported in cases of rumination [58], which may be seen as a purely cognitive activity associated with

depression. This could be correlated with the brain-to-LF changes reported in cases of mild depression [32], using the same BHI estimation model.

It is worth noting that brain-to-heart variations appear to be smoother across the scalp and the considered EEG frequency bands, whereas the heart-to-brain interplay exhibits a higher spatial-specific response (see Fig. 5a). Previous studies have hypothesized that this might be attributed to a more diffuse brain-to-heart interaction, while the brain's response to heart activity may be more spatially and temporally localized [28,59].

This study has some limitations. Firstly, the BHI quantification is a relatively novel topic where a generalized consensus on a standard technique has not been achieved yet. Indeed, while the physiologically-plausible SDG model utilized in this study seems the best methodological choice to investigate test anxiety, it would be interesting to perform further assessments of functional BHI using additional methodological tools (e.g., [21,22,26,28]). Secondly, the study considered a limited cohort and despite being a multi-system study, it does not account for potential information from respiration dynamics. Indeed, functional BHI may be influenced by respiration [60], since it might affect autonomic interactions acting on the baroreflex [61] and cerebral autoregulation [62]. Future studies will aim for a more comprehensive modeling of CNS-ANS interaction, taking into account respiratory influence [11,12]. Moreover, while this study relies on the classical LF-HF spectral division of cardiovascular variability series, such a net division has been debated due to the non-specificity of related sympathovagal correlates [63]. Future work should focus on properly disentangling sympathetic and vagal activity while evaluating functional BHI [57]. Specific paradigmatic BHI oscillations around 0.15 Hz should however be further investigated, since this frequency has been highlighted as "central pacemaker" in different studies investigating brain- and brain-heart dynamics [64–67]. Furthermore, it will be relevant to investigate functional BHI in anxiety by considering the minimalization of the energy demand due to synchronization of brain and body rhythms [68] and the slowest shared resonance [69].

4.1. Conclusions

The brain-heart axis dynamics provides a comprehensive framework for understanding the multisystem physiological response to induced test anxiety. Experimental findings elucidate the simultaneous and coordinated operation of both the central and autonomic nervous systems, and how their interaction is shaped by test anxiety. Anticipatory test anxiety during a study phase predominantly impacts heart-to-brain activity across a broad cardiac frequency range and extensive cortical regions. In contrast, anxiety arising from interrogation primarily affects brain-to-heart activity, focusing on low-frequency cardiac activity originating from specific cortical areas.

CRediT authorship contribution statement

Vincenzo Catrambone: Conceptualization, Data curation, Formal analysis, Investigation, Methodology, Software, Writing – original draft, Writing – review & editing. **Lorenzo Zallocco:** Data curation, Writing – review & editing. **Eleonora Ramoretti:** Data curation, Writing – review & editing. **Maria Rosa Mazzoni:** Data curation, Resources, Writing – review & editing. **Laura Sebastiani:** Conceptualization, Data curation, Funding acquisition, Investigation, Project administration, Supervision, Writing – review & editing. **Gaetano Valenza:** Conceptualization, Data curation, Funding acquisition, Methodology, Writing – review & editing.

Declaration of competing interest

The authors declare that they have no known competing financial interests or personal relationships that could have appeared to influence the work reported in this paper.

References

[1] L. Fehm, A. Pelissolo, T. Furmark, H.-U. Wittchen, Size and burden of social phobia in europe, Eur. Neuropsychopharmacol. 15 (4) (2005) 453–462.
[2] A.S. Morrison, R.G. Heimberg, Social anxiety and social anxiety disorder, Annu. Rev. Clin. Psychol. 9 (2013) 249–274.
[3] M.B. Stein, D.J. Stein, Social anxiety disorder, The Lancet 371 (9618) (2008) 1115–1125.
[4] N.A. Heiser, S.M. Turner, D.C. Beidel, R. Roberson-Nay, Differentiating social phobia from shyness, J. Anxiety Disord. 23 (4) (2009) 469–476.
[5] M. Zeidner. Test anxiety: the state of the art, Plenum, New York, 1998.
[6] C.D. Spielberger, P.R. Vagg, Test Anxiety: Theory, Assessment, and Treatment, Taylor & Francis, 1995.
[7] M. Zeidner, G. Matthews, R.D. Roberts, The emotional intelligence, health, and well-being nexus: what have we learned and what have we missed? Appl. Psychol. Health Well-Being 4 (1) (2012) 1–30.
[8] R.M. Liebert, L.W. Morris, Cognitive and emotional components of test anxiety: a distinction and some initial data, Psychol. Rep. 20 (3) (1967) 975–978.
[9] D.L. Bandalos, K. Yates, T. Thorndike-Christ, Effects of math self-concept, perceived self-efficacy, and attributions for failure and success on test anxiety, J. Educ. Psychol. 87 (4) (1995) 611.
[10] J. Goheen, J.A. Anderson, J. Zhang, G. Northoff, From lung to brain: respiration modulates neural and mental activity, Neurosci. Bull. (2023) 1–14.
[11] Ł. Dziuda, P. Zieliński, P. Baran, M. Krej, L. Kopka, A study of the relationship between the level of anxiety declared by MRI patients in the STAI questionnaire and their respiratory rate acquired by a fibre-optic sensor system, Sci. Rep. 9 (1) (2019) 4341.
[12] G. Pfurtscheller, M. Kaminski, K. J. Blinowska, B. Rassler, G. Schwarz, W. Klimesch, Respiration-entrained brain oscillations in healthy fMRI participants with high anxiety, Sci. Rep. 13 (1) (2023) 2380.
[13] M.F. Detweiler, J.S. Comer, K.I. Crum, A.M. Albano, Social anxiety in children and adolescents: biological, developmental, and social considerations. Social Anxiety, Elsevier, 2014, pp. 253–309.
[14] J.D. Caouette, A.E. Guyer, Gaining insight into adolescent vulnerability for social anxiety from developmental cognitive neuroscience, Dev. Cognit. Neurosci. 8 (2014) 65–76.
[15] Y.-H. Jung, J.E. Shin, Y.I. Lee, J.H. Jang, H.J. Jo, S.-H. Choi, Altered amygdala resting-state functional connectivity and hemispheric asymmetry in patients with social anxiety disorder, Front. Psychiatry 9 (2018) 164.
[16] K.E. Prater, A. Hosanagar, H. Klumpp, M. Angstadt, K. Luan Phan, Aberrant amygdala–frontal cortex connectivity during perception of fearful faces and at rest in generalized social anxiety disorder, Depression Anxiety 30 (3) (2013) 234–241.
[17] A.S. Fox, N.H. Kalin, A translational neuroscience approach to understanding the development of social anxiety disorder and its pathophysiology, Am. J. Psychiatry 171 (11) (2014) 1162–1173.
[18] C.S. Monk, E.E. Nelson, E.B. McClure, K. Mogg, B.P. Bradley, E. Leibenluft, R.J. R. Blair, G. Chen, D.S. Charney, M. Ernst, et al., Ventrolateral prefrontal cortex activation and attentional bias in response to angry faces in adolescents with generalized anxiety disorder, Am. J. Psychiatry 163 (6) (2006) 1091–1097.
[19] G. Valenza, R. Sclocco, A. Duggento, L. Passamonti, V. Napadow, R. Barbieri, N. Toschi, The central autonomic network at rest: uncovering functional MRI correlates of time-varying autonomic outflow, Neuroimage 197 (2019) 383–390.
[20] V. Catrambone, G. Valenza, Functional Brain-Heart Interplay, Springer, 2021.
[21] L. Faes, D. Marinazzo, S. Stramaglia, F. Jurysta, A. Porta, N. Giandomenico, Predictability decomposition detects the impairment of brain–heart dynamical networks during sleep disorders and their recovery with treatment, Philos. Trans. R. Soc. A Math. Phys. Eng. Sci. 374 (2067) (2016) 20150177.
[22] L. Faes, D. Marinazzo, F. Jurysta, G. Nollo, Linear and non-linear brain–heart and brain–brain interactions during sleep, Physiol. Meas. 36 (4) (2015) 683.
[23] V. Catrambone, A. Talebi, R. Barbieri, G. Valenza, Time-resolved brain-to-heart probabilistic information transfer estimation using inhomogeneous point-process models, IEEE Trans. Biomed. Eng. 68 (11) (2021) 3366–3374.
[24] H. Al-Nashash, Y. Al-Assaf, J. Paul, N. Thakor, EEG signal modeling using adaptive Markov process amplitude, IEEE Trans. Biomed. Eng. 51 (5) (2004) 744–751.
[25] V. Catrambone, R. Barbieri, H. Wendt, P. Abry, G. Valenza, Functional brain–heart interplay extends to the multifractal domain, Philos. Trans. R. Soc. A 379 (2212) (2021) 20200260.
[26] A. Porta, A. Fantinato, V. Bari, B. Cairo, B. De Maria, E.G. Bertoldo, V. Fiolo, E. Callus, C. De Vincentiis, M. Volpe, et al., Complexity and nonlinearities of short-term cardiovascular and cerebrovascular controls after surgical aortic valve replacement. 2020 42nd Annual International Conference of the IEEE Engineering in Medicine & Biology Society (EMBC), IEEE, 2020, pp. 2569–2572.
[27] V. Catrambone, G. Valenza, Complex brain-heart mapping in mental and physical stress, IEEE J. Transl. Eng. Health Med. (2023).
[28] V. Catrambone, G. Valenza, Microstates of the cortical brain-heart axis, Hum. Brain Mapp. 44 (17) (2023) 5846–5857.
[29] V. Catrambone, A. Greco, N. Vanello, E.P. Scilingo, G. Valenza, Time-resolved directional brain–heart interplay measurement through synthetic data generation models, Ann. Biomed. Eng. 47 (2019) 1479–1489.
[30] D. Candia-Rivera, V. Catrambone, J.F. Thayer, C. Gentili, G. Valenza, Cardiac sympathetic-vagal activity initiates a functional brain–body response to emotional arousal, Proc. Natl. Acad. Sci. 119 (21) (2022).e2119599119
[31] V. Catrambone, G. Valenza, Nervous–system–wise functional estimation of directed brain–heart interplay through microstate occurrences, IEEE Trans. Biomed. Eng. 70 (8) (2023) 2270–2278.

[32] V. Catrambone, S. Messerotti Benvenuti, C. Gentili, G. Valenza, Intensification of functional neural control on heartbeat dynamics in subclinical depression, Transl. Psychiatry 11 (1) (2021) 221.
[33] V. Miskovic, A.R. Ashbaugh, D.L. Santesso, R.E. McCabe, M.M. Antony, L. A. Schmidt, Frontal brain oscillations and social anxiety: a cross-frequency spectral analysis during baseline and speech anticipation, Biol. Psychol. 83 (2) (2010) 125–132.
[34] L.J. Gabard-Durnam, A.S. Mendez Leal, C.L. Wilkinson, A.R. Levin, The harvard automated processing pipeline for electroencephalography (HAPPE): standardized processing software for developmental and high-artifact data, Front. Neurosci. 12 (2018) 97.
[35] A. Delorme, S. Makeig, EEGLAB: an open source toolbox for analysis of single-trial eeg dynamics including independent component analysis, J. Neurosci. Methods 134 (1) (2004) 9–21.
[36] J. Pan, W.J. Tompkins, A real-time QRS detection algorithm, IEEE Trans. Biomed. Eng. (3) (1985) 230–236.
[37] L. Citi, E.N. Brown, R. Barbieri, A real-time automated point-process method for the detection and correction of erroneous and ectopic heartbeats, IEEE Trans. Biomed. Eng. 59 (10) (2012) 2828–2837.
[38] M. Brennan, M. Palaniswami, P. Kamen, Poincaré plot interpretation using a physiological model of HRV based on a network of oscillators, Am. J. Physiol.-Heart Circ. Physiol. 283 (5) (2002) H1873–H1886.
[39] V. Catrambone, 2019, https://it.mathworks.com/matlabcentral/fileexchange/72704-brain-heart-interaction-indexes.
[40] A. Porta, L. Faes, Wiener–Granger causality in network physiology with applications to cardiovascular control and neuroscience, Proc. IEEE 104 (2) (2015) 282–309.
[41] K.J. Friston, et al., Assessing the significance of focal activations using their spatial extent, Hum. Mapp. 1 (3) (1994) 210–220.
[42] L. Zallocco, L. Giusti, M. Ronci, A. Mussini, M. Trerotola, M.R. Mazzoni, A. Lucacchini, L. Sebastiani, Salivary proteome changes in response to acute psychological stress due to an oral exam simulation in university students: effect of an olfactory stimulus, Int. J. Mol. Sci. 22 (9) (2021) 4295.
[43] J.F. Thayer, F. Åhs, M. Fredrikson, J.J. Sollers III, T.D. Wager, A meta-analysis of heart rate variability and neuroimaging studies: implications for heart rate variability as a marker of stress and health, Neurosci. Biobehav. Rev. 36 (2) (2012) 747–756.
[44] J.F. Thayer, A.L. Hansen, E. Saus-Rose, B.H. Johnsen, Heart rate variability, prefrontal neural function, and cognitive performance: the neurovisceral integration perspective on self-regulation, adaptation, and health, Ann. Behav. Med. 37 (2) (2009) 141–153.
[45] L. Bernardi, J. Wdowczyk-Szulc, C. Valenti, S. Castoldi, C. Passino, G. Spadacini, P. Sleight, Effects of controlled breathing, mental activity and mental stress with or without verbalization on heart rate variability, J. Am. Coll. Cardiol. 35 (6) (2000) 1462–1469.
[46] A. Brugnera, C. Zarbo, M.P. Tarvainen, P. Marchettini, R. Adorni, A. Compare, Heart rate variability during acute psychosocial stress: a randomized cross-over trial of verbal and non-verbal laboratory stressors, Int. J. Psychophysiol. 127 (2018) 17–25.
[47] J.T. Cacioppo, B.N. Uchino, G.G. Berntson, Individual differences in the autonomic origins of heart rate reactivity: the psychometrics of respiratory sinus arrhythmia and preejection period, Psychophysiology 31 (4) (1994) 412–419.
[48] A. Hernando, J. Lazaro, E. Gil, A. Arza, J.M. Garzón, R. Lopez-Anton, C. De La Camara, P. Laguna, J. Aguiló, R. Bailón, Inclusion of respiratory frequency information in heart rate variability analysis for stress assessment, IEEE J. Biomed. Health Inform. 20 (4) (2016) 1016–1025.
[49] C. Zelano, H. Jiang, G. Zhou, N. Arora, S. Schuele, J. Rosenow, J.A. Gottfried, Nasal respiration entrains human limbic oscillations and modulates cognitive function, J. Neurosci. 36 (49) (2016) 12448–12467.
[50] L. Henke, A.G. Lewis, L. Meyer, Fast and slow rhythms of naturalistic reading revealed by combined eye-tracking and electroencephalography, J. Neurosci. 43 (24) (2023) 4461–4469.
[51] L. Dugué, P. Marque, R. VanRullen, Theta oscillations modulate attentional search performance periodically, J. Cognit. Neurosci. 27 (5) (2015) 945–958.
[52] R. Michel, L. Dugué, N.A. Busch, Distinct contributions of alpha and theta rhythms to perceptual and attentional sampling, Eur. J. Neurosci. 55 (11–12) (2022) 3025–3039.
[53] A.N. Landau, H.M. Schreyer, S. Van Pelt, P. Fries, Distributed attention is implemented through theta-rhythmic gamma modulation, Curr. Biol. 25 (17) (2015) 2332–2337.
[54] B.M. Roberts, A. Clarke, R.J. Addante, C. Ranganath, Entrainment enhances theta oscillations and improves episodic memory, Cognit. Neurosci. 9 (3–4) (2018) 181–193.
[55] G.G. Knyazev, A.N. Savostyanov, E.A. Levin, Anxiety and synchrony of alpha oscillations, Int. J. Psychophysiol. 57 (3) (2005) 175–180.
[56] I. Palacios-García, J. Silva, M. Villena-González, G. Campos-Arteaga, C. Artigas-Vergara, N. Luarte, E. Rodríguez, C.A. Bosman, Increase in beta power reflects attentional top-down modulation after psychosocial stress induction, Front. Hum. Neurosci. 15 (2021) 630813.
[57] D. Candia-Rivera, V. Catrambone, R. Barbieri, G. Valenza, Functional assessment of bidirectional cortical and peripheral neural control on heartbeat dynamics: a brain-heart study on thermal stress, NeuroImage 251 (2022) 119023.
[58] L. Carnevali, J.F. Thayer, J.F. Brosschot, C. Ottaviani, Heart rate variability mediates the link between rumination and depressive symptoms: a longitudinal study, Int. J. Psychophysiol. 131 (2018) 131–138.
[59] O. Pollatos, W. Kirsch, R. Schandry, Brain structures involved in interoceptive awareness and cardioafferent signal processing: a dipole source localization study, Hum. Brain Mapp. 26 (1) (2005) 54–64.
[60] A. Zaccaro, M.G. Perrucci, E. Parrotta, M. Costantini, F. Ferri, Brain-heart interactions are modulated across the respiratory cycle via interoceptive attention, Neuroimage 262 (2022) 119548.
[61] A. Porta, T. Bassani, V. Bari, G.D. Pinna, R. Maestri, S. Guzzetti, Accounting for respiration is necessary to reliably infer Granger causality from cardiovascular variability series, IEEE Trans. Biomed. Eng. 59 (3) (2011) 832–841.
[62] A. Porta, F. Gelpi, V. Bari, B. Cairo, B. De Maria, D. Tonon, G. Rossato, M. Ranucci, L. Faes, Categorizing the role of respiration in cardiovascular and cerebrovascular variability interactions, IEEE Trans. Biomed. Eng. 69 (6) (2021) 2065–2076.
[63] G. Valenza, L. Citi, J.P. Saul, R. Barbieri, Measures of sympathetic and parasympathetic autonomic outflow from heartbeat dynamics, J. Appl. Physiol. 125 (1) (2018) 19–39.
[64] G. Pfurtscheller, K.J. Blinowska, M. Kaminski, B. Rassler, W. Klimesch, Processing of fMRI-related anxiety and information flow between brain and body revealed a preponderance of oscillations at 0.15/0.16 Hz, Sci. Rep. 12 (1) (2022) 9117.
[65] D.S. Kluger, J. Gross, Depth and phase of respiration modulate cortico-muscular communication, Neuroimage 222 (2020) 117272.
[66] V. Perlitz, B. Cotuk, M. Lambertz, R. Grebe, G. Schiepek, E. Petzold, H. Schmid-Schönbein, G. Flatten, Coordination dynamics of circulatory and respiratory rhythms during psychomotor drive reduction, Auton. Neurosci. 115 (1–2) (2004) 82–93.
[67] G. Pfurtscheller, A.R. Schwerdtfeger, B. Rassler, A. Andrade, G. Schwarz, W. Klimesch, Verification of a central pacemaker in brain stem by phase-coupling analysis between hr interval-and bold-oscillations in the 0.10–0.15 Hz frequency band, Front. Neurosci. 14 (2020) 922.
[68] W. Klimesch, The frequency architecture of brain and brain body oscillations: an analysis, Eur. J. Neurosci. 48 (7) (2018) 2431–2453.
[69] A. Young, T. Hunt, M. Ericson, The slowest shared resonance: a review of electromagnetic field oscillations between central and peripheral nervous systems, Front. Hum. Neurosci. 15 (2022) 796455.